PHYSICAL REVIEW B **78**, 220405(R) (2008)

Spin correlations in the geometrically frustrated pyrochlore $Tb_2Mo_2O_7$

D. K. Singh,[1] J. S. Helton,[1] S. Chu,[2] T. H. Han,[1] C. J. Bonnoit,[1] S. Chang,[3,4] H. J. Kang,[3,4] J. W. Lynn,[3] and Y. S. Lee[1]
[1]*Department of Physics, Massachusetts Institute of Technology, Cambridge, Massachusetts 02139, USA*
[2]*Center for Materials Science and Engineering, Massachusetts Institute of Technology, Cambridge, Massachusetts 02139, USA*
[3]*NIST Center for Neutron Research, Gaithersburg, Maryland 20899, USA*
[4]*Department of Materials Science and Engineering, University of Maryland, College Park, Maryland 20742, USA*
(Received 20 October 2008; published 31 December 2008)

We report neutron-scattering studies of the spin correlations of the geometrically frustrated pyrochlore $Tb_2Mo_2O_7$ using single-crystal samples. This material undergoes a spin-freezing transition below $T_g \simeq 24$ K, similar to $Y_2Mo_2O_7$, and has little apparent chemical disorder. Diffuse elastic peaks are observed at low temperatures, indicating short-range ordering of the Tb moments in an arrangement where the Tb moments are slightly rotated from the preferred directions of the spin-ice structure. In addition, a $\vec{Q}$-independent signal is observed which likely originates from frozen but completely uncorrelated Tb moments. Inelastic measurements show the absence of sharp peaks due to crystal-field excitations. These data show how the physics of the Tb sublattice responds to the glassy behavior of the Mo sublattice with the associated effects of lattice disorder.

DOI: 10.1103/PhysRevB.78.220405 PACS number(s): 75.25.+z, 75.40.Gb, 75.50.Lk, 78.70.Nx

Geometrically frustrated magnets can exhibit unusual phenomena at low temperatures such as spin-glass,[1,2] spin-ice,[3–5] and spin liquid[6,7] states. The frustrated pyrochlore compound $Tb_2Mo_2O_7$ stands at an interesting crossroads, being a representative of both the Mo-based family $R_2Mo_2O_7$ (R=rare earth) and other Tb-based compounds $Tb_2M_2O_7$ (M=metal). As a function of the R-site radius, the $R_2Mo_2O_7$ compounds exhibit a metal-insulator transition between ferromagnetic metal states and spin-glass insulators.[8,9] The ferromagnetic metals (such as $Nd_2Mo_2O_7$ and $Sm_2Mo_2O_7$) show an interesting interplay between the spin configuration and the transport properties, which can give rise to anomalous Hall and Nernst signals.[10,11] The spin-glass insulators (such as $Y_2Mo_2O_7$ and $Tb_2Mo_2O_7$) have generated much interest due to the apparent lack of chemical disorder and the relation to geometrical frustration.[1,2] Outside of the Mo family, pyrochlore compounds with Tb as the rare earth have been extensively studied because the combination of exchange and dipolar interactions coupled with moderate spin anisotropy can lead to various ground states depending on the metal ion. For example, $Tb_2Ti_2O_7$ has a spin liquid ground state,[6] while $Tb_2Sn_2O_7$ exhibits magnetic order[12] and both show persistent spin dynamics down to the lowest measured temperatures.[6,13,14]

$Tb_2Mo_2O_7$ crystallizes in the $Fd\bar{3}m$ cubic space group and both the Tb and Mo sublattices form three-dimensional networks of corner sharing tetrahedra. Spin freezing is observed below $T_g \simeq 24$ K and diffuse scattering from the Tb moments has been observed with neutron scattering on powder samples.[1,15,16] Remarkably, the spins keep fluctuating down to the lowest temperatures measured in muon spin rotation (μSR) studies.[17] Currently, the spin structure of the short-range order is not known, nor has there been a precise determination of the correlation lengths. Also, not much is known about the possible effects of disorder if present. This Rapid Communication presents results from neutron-scattering measurements on a single crystal which address some of these questions.

Single-crystal samples of $Tb_2Mo_2O_7$ were grown using the floating-zone technique in an image furnace. A mixture of Tb_4O_7 (99.97%) and MoO_2 (99.99%) was thoroughly ground and pressed into feed rods and the crystal growth was carried out in an Ar atmosphere. The samples were confirmed to be single phase $Tb_2Mo_2O_7$ by x-ray and neutron diffraction. The magnetic susceptibility shown in the inset of Fig. 1(a) is consistent with previous results on powders. The difference between the zero-field-cooled (ZFC) and field-cooled (FC) susceptibilities indicate a spin-freezing temperature of $T_g \simeq 24$ K. Fitting the high-temperature susceptibility data ($T > 100$ K) to a Curie-Weiss law yields a Curie-Weiss temperature of $\Theta_{CW} \simeq 12$ K and an effective moment of $\sim 9.5\ \mu_B$. The size of the moment is consistent with large Tb^{3+} moments[18] dominating the response. The nature of the magnetic couplings is not so clear; currently, the values of the Tb-Tb, Tb-Mo, and Mo-Mo interactions in $Tb_2Mo_2O_7$ are not known. In $Y_2Mo_2O_7$ (where Y is nonmagnetic), the Curie-Weiss temperature of about -200 K suggests that the Mo-Mo interaction is strongly antiferromagnetic.[2] $Y_2Mo_2O_7$ has a spin-freezing temperature ($T_g \simeq 22.5$ K) similar to that in $Tb_2Mo_2O_7$. Neutron measurements on $Y_2Mo_2O_7$ have shown that dynamical short-range order of the Mo sublattice develops below room temperature.[2] To better understand how the Tb^{3+} ions respond to the glassy behavior of the Mo sublattice, we have carried out a series of neutron-scattering measurements.

The neutron experiments were performed using a 0.49 g single crystal of $Tb_2Mo_2O_7$ at the NIST Center for Neutron Research. The spin-polarized triple-axis spectrometer (SPINS) and BT9 triple axis spectrometers were used with fixed final neutron energies of 4.5 and 14.7 meV, respectively. At SPINS, we employed the horizontally focused analyzer with collimator sequence 80′-sample-Be-radial open. At BT9, a flat analyzer was used with collimations 40′–48′-PG-sample-40′–90′ (PG stands for pyrolitic graphite). The crystal was oriented in the (HHL) zone and placed in a ^{4}He cryostat.

On SPINS, we observed the onset of diffuse elastic peaks upon cooling and representative scans through the (002) and (111) positions are shown in Figs. 1(b) and 1(c). At T =1.5 K, the peak widths are large, spanning a considerable fraction of the Brillioun zone indicating short-range order.

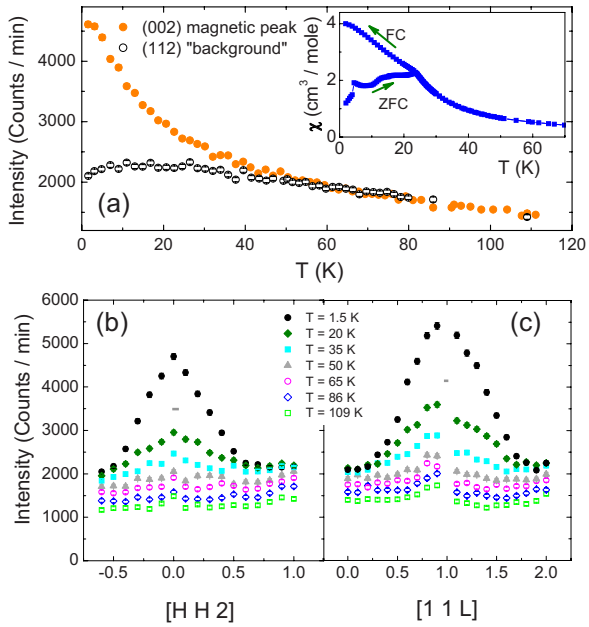

FIG. 1. (Color online) Elastic scattering measured on SPINS spectrometer. (a) Intensity at the (002) diffuse magnetic peak position and the "background" signal measured at the (112) position as a function of temperature. Inset: Magnetic susceptibility measured with $H=10$ Oe along the [111] direction using a superconducting quantum interference device (SQUID) magnetometer. Scans through the (b) (002) position and the (c) (111) position at various temperatures. The horizontal bar indicates the instrumental resolution.

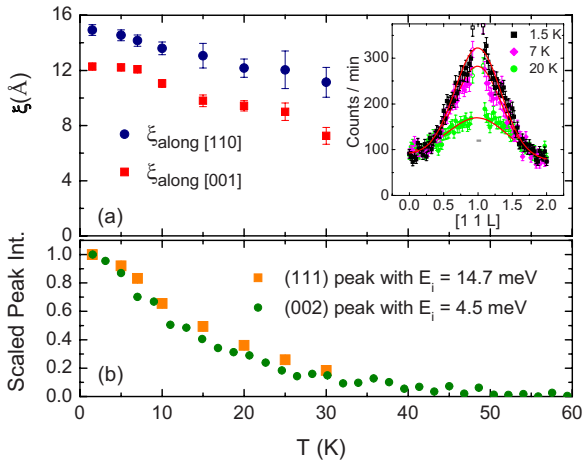

FIG. 2. (Color online) (a) Correlation lengths of the short-range order along different symmetry directions as a function of temperature. Inset: Representative scans through the (111) position measured on the BT9 spectrometer, where the horizontal bar indicates the instrumental resolution. (b) Temperature dependence of the diffuse peak intensities.

Since the magnitude of the Tb moment should be about five times larger than the Mo moment, we identify these peaks as arising from short-range order on the Tb sublattice. The intensity at the (002) diffuse peak position is plotted as a function of temperature in Fig. 1(a), and the "background" signal measured at (112) is also plotted. The onset of the diffuse peak intensity occurs around $T \sim 2\ T_g$ and increases smoothly upon cooling through T_g. This is similar to the temperature dependence of elastic scattering observed for $Y_2Mo_2O_7$,[2] indicating that the Tb correlations are coupled to the developing Mo correlations.

In addition, we find a significant temperature dependence of the $\vec{Q}$-independent "background" signal in $Tb_2Mo_2O_7$. Cooling from $T=109$ K to around 50 K, the intensity at (112) increases roughly linearly with decreasing temperature. The $\vec{Q}$ independence of the signal can clearly be seen in the scans in Figs. 1(b) and 1(c). Typically, $\vec{Q}$-independent background processes produce scattering which increases with increasing temperature, which is the opposite of what we observe. A likely origin of this $\vec{Q}$-independent scattering is the presence of frozen Tb moments which are completely uncorrelated. This identification is supported by the flattening of the temperature dependence below ~30 K, which is the same temperature at which the peaks due to correlated Tb moments begin to rise quickly. Such $\vec{Q}$-independent scattering from Tb is unusual and may be caused by their coupling to the slowly fluctuating Mo moments as discussed further below. We find that both the diffuse peaks and the $\vec{Q}$-independent signal are resolution limited in energy. Although the energy resolution was narrow ($\Delta E \simeq 0.12$ meV), fluctuations at a rate below ~0.02 THz would be indistinguishable from being static.

Further elastic measurements were performed on BT9 and representative scans through the (111) peak are shown in the inset of Fig. 2(a). The solid lines indicate fits to Gaussian line shapes plus a sloping background. The sharp nuclear Bragg peaks denoted by the open symbols were not included in the fits. Scans were performed along the H, H, and L directions to determine the static correlation lengths as functions of temperature. Interpreting the Gaussian linewidths within a finite-size domain model, we calculated the correlation lengths ξ (or linear domain sizes) as plotted in Fig. 2(a). The correlations are not completely isotropic, with $\xi_{\text{along}[110]}$ slightly larger than $\xi_{\text{along}[001]}$. Both correlation lengths increase modestly upon cooling and span a distance of roughly the size of a unit cell. Again, no dramatic changes are observed at T_g. The fitted peak intensities are plotted in Fig. 2(b), and the temperature dependence closely follows that of the previous data taken with 4.5 meV neutrons which have higher-energy resolution.

An important issue is to understand the local structure of the correlated Tb moments. In Fig. 3(a) we show the pattern of the elastic-scattering intensity in the (HHL)-zone spanning a wide region of reciprocal space using 14.7 meV neutrons taken at $T=1.5$ K. Compared to previous powder measurements,[15,16] the single-crystal data allow for a much more detailed examination of the intensities. The previously observed broad peak in the powder at $|\vec{Q}| \sim 1$ Å^{-1} is consistent with contributions from the [111] and [002] diffuse peaks and the powder peak at 2 Å^{-1} with the [222] and [113] diffuse peaks. To the first approximation, the peaks appear at positions consistent with a $\vec{Q}=0$ arrangement (consisting of equivalent tetrahedra with moments along the local [111] anisotropy axes with a "two-in and two-out" arrangement).[4,5]

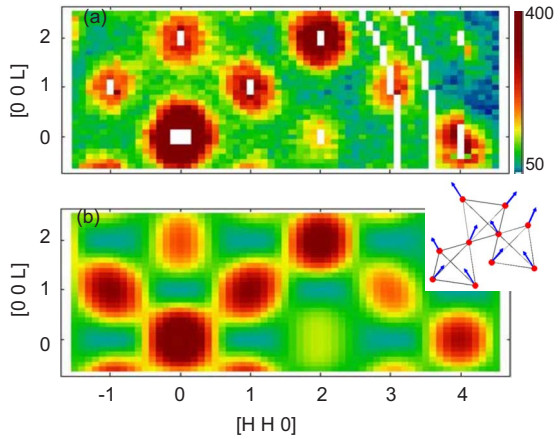

FIG. 3. (Color online) (a) Pattern of the elastic-scattering intensity at $T=1.5$ K measured on BT9 in the (HHL) zone. Data points due to scattering from nuclear Bragg peaks and Al powder lines (indicated by white regions) were removed in order to emphasize the diffuse magnetic scattering. (b) Calculated scattering pattern for short-range-ordered regions with the spin structure shown in the inset, which are domain averaged as described in the text. A constant background of 60 counts (which approximates the average background in the data) was added to the calculation.

However, a closer inspection of the intensities suggests deviations from the local spin-ice structure. We calculated the magnetic scattering cross section for various spin configurations on a small cluster of four Tb tetrahedra. A close match was achieved with an arrangement in which all tetrahedra in the cluster are identical and the Tb moments are rotated away from the local [111] anisotropy axes of the spin-ice configuration by 14°. A depiction of this local order is shown in the inset of Fig. 3(b). The rotation of the Tb moments enhances the net ferromagnetic moment along the [001] direction for each tetrahedra. Since there are six equivalent domains for this spin structure, our calculation averages over all six magnetic domains. The uniform susceptibility data rule out a net ferromagnetic moment at low temperatures, hence the ferromagnetic moment from each cluster must cancel overall consistent with our domain-averaged cross section. The calculated cross section plotted in Fig. 3(b) shows reasonably good agreement with the data. We estimate that the static moment associated with the diffuse peaks at $T=1.6$ K is $\langle M_{\mathrm{Tb}}\rangle \simeq 4.0(5)\mu_B$, significantly smaller than that expected for a free Tb^{3+} ion, which may partly be explained by crystal-field effects.[18,19] This may also indicate that a substantial fraction of the Tb moment remains dynamic or is frozen without measurable spatial correlations. We comment more on the latter possibility below. Interestingly, our model for the local spin structure is similar to the long-range order of Tb moments observed in diluted $Tb_{1.8}La_{0.2}Mo_2O_7$ which is a ferromagnet at low temperatures.[16] By analogy to the diluted compounds, it is possible that the Mo moments are correlated within each short-range-ordered cluster. However, since the measured intensity pattern is well described by a simple Tb-only model, we presently cannot deduce the presence of Mo sublattice ordering. There are also similarities to the Tb order found in the ferromagnetic state of $Tb_2Sn_2O_7$,[12,20] even though $Tb_2Mo_2O_7$ is a short-range-ordered spin glass.

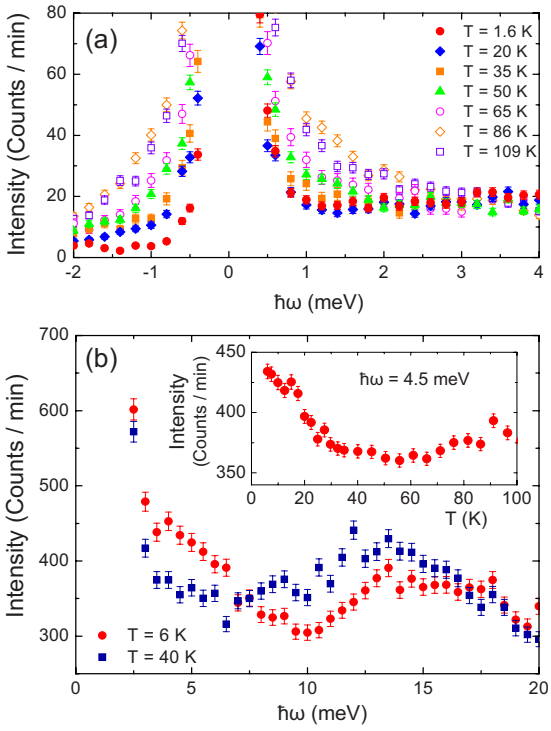

FIG. 4. (Color online) Inelastic-scattering data. (a) High-resolution measurements taken on SPINS at the (1.1, 1.1, 1) position in a single crystal. (b) Higher-energy data taken on the BT7 spectrometer (with $E_f=14.7$ meV and horizontally focused analyzer) on a powder sample at $|\vec{Q}|=3$ Å^{-1}. Inset: Temperature dependence of the scattering at $\hbar\omega=4.5$ meV.

Finally, we performed inelastic-scattering measurements to investigate the Tb crystal-field excitations, as well as possible collective excitations. In the structurally similar $Tb_2Ti_2O_7$ and $Tb_2Sn_2O_7$ compounds, a low-lying crystal-field excitation has been observed near 1.5 meV. This corresponds to an excitation from the ground-state doublet to the first-excited state. Surprisingly, in $Tb_2Mo_2O_7$, we do not observe a sharp mode corresponding to this excitation. Figure 4(a) shows energy scans taken at the (1.1, 1.1, 1) position on the SPINS spectrometer. Data taken at the (001) position (not shown) yield similar spectra. At $T=1.6$ K, the data for positive-energy transfers reveal a rather flat fluctuation spectrum without a clear peak in the range between 0.5 and 4 meV. Warming to 20 K produces very little change, though further warming results in additional low-energy quasielastic scattering consistent with previous observations.[15] The growth of this quasielastic scattering appears to correlate with the diminishment of the $\vec{Q}$-independent elastic signal. Inelastic scans were also performed at higher-energy transfers (up to $\hbar\omega=20$ meV) on a 2.46 g powder sample of $Tb_2Mo_2O_7$ using the BT7 spectrometer, as shown in Fig. 4(b). No sharp peaks associated with crystal-field excitations are observed, though the low-temperature spectrum shows broad features centered around 4 and 15 meV. In contrast, both $Tb_2Ti_2O_7$ and $Tb_2Sn_2O_7$ exhibit sharp crystal-field excitations at about 10 and 15 meV.[6,19]

The lack of sharp crystal-field excitations for Tb^{3+} in $Tb_2Mo_2O_7$ is unexpected and requires better understanding.

One possible origin may be a static inhomogeneous splitting of the non-Kramers Tb^{3+} doublet due to lattice strains. Such an effect has been observed in $Pr_{2-x}Bi_xRu_2O_7$ which has obvious chemical disorder.[21] While structural disorder has not yet been identified in $Tb_2Mo_2O_7$, recent experiments on the $Y_2Mo_2O_7$ compound reveal that there exists lattice disorder associated with the Mo-Mo bond distances.[22,23] Since $Tb_2Mo_2O_7$ has a similar spin-freezing transition, it is reasonable to expect similar levels of Mo sublattice disorder. This would produce some degree of inhomogeneity in the Tb crystal-field environments, thereby broadening the excitations. Another effect to consider is the interaction of the slowly fluctuating Mo moments with the Tb moments. Freezing of the Mo moments manifestly breaks time-reversal symmetry, and therefore any coupling with the Tb sublattice would split the ground-state Tb^{3+} doublet. The magnitude of the splitting would depend on the mean field generated by the local configuration of Mo moments. Assuming the Tb^{3+} ground-state doublet is primarily $|\pm 4\rangle$ or $|\pm 5\rangle$, as seen in related Tb pyrochlores,[18,19] then the mean field at the Tb site due to the neighboring Mo would select a preferred local spin direction. As the Mo moments gradually become frozen in a disordered arrangement, the net effect on the Tb sublattice would be to select $|+J_z\rangle$ or $|-J_z\rangle$ in a spatially disordered way. Such a frozen and uncorrelated Tb configuration would appear as a $\vec{Q}$-independent background consistent with our observations from the elastic-scattering measurements. Indeed, the presence of static but uncorrelated Tb moments would naturally explain the relatively small value of $\langle M_{\mathrm{Tb}}\rangle$ calculated from the diffuse peak intensities, since a significant fraction of the elastic signal would be $\vec{Q}$ independent.

In Fig. 4(b), the inelastic spectrum at $T=6$ K of the powder sample exhibits enhanced scattering centered around 4 meV which quickly diminishes upon warming to above ~30 K (see the inset). The temperature dependence closely follows that of the diffuse elastic peaks. This behavior suggests that the enhanced scattering around 4 meV is derived from collective excitations of the Tb moments rather than single-ion physics. The energy for this collective excitation should thus be related to a combination of the Tb-Tb and Tb-Mo interaction energy scales. Further inelastic studies on the single-crystal sample would be necessary to specify the magnitudes of the different interactions.

In conclusion, neutron-scattering studies on a single crystal of $Tb_2Mo_2O_7$ reveal two components to the elastic scattering: a set of diffuse peaks plus a $\vec{Q}$-independent signal. The short-range order of the Tb moments has been identified and the observed correlation lengths are slightly anisotropic. The inelastic data indicate that the physics of the Tb sublattice is affected by disorder, most likely through lattice inhomogeneity and through coupling to the glassy Mo moments. Further inelastic studies to determine the Tb-Mo interaction would shed light on the latter possibility. This also points to the importance of future work to investigate the degree of structural inhomogeneity in these samples.

We thank T. Senthil, S. Speakman, and Y. Chen for useful discussions. The work at MIT was supported by the Department of Energy (DOE) under Grant No. DE-FG02-07ER46134. This work used facilities supported in part by the NSF under Agreement No. DMR-0454672.

[1] J. E. Greedan, J. N. Reimers, C. V. Stager, and S. L. Penny, Phys. Rev. B **43**, 5682 (1991).
[2] J. S. Gardner, B. D. Gaulin, S. H. Lee, C. Broholm, N. P. Raju, and J. E. Greedan, Phys. Rev. Lett. **83**, 211 (1999).
[3] A. P. Ramirez, A. Hayashi, R. J. Cava, R. Siddharthan, and B. S. Shastry, Nature (London) **399**, 333 (1999).
[4] M. J. Harris, S. T. Bramwell, D. F. McMorrow, T. Zeiske, and K. W. Godfrey, Phys. Rev. Lett. **79**, 2554 (1997).
[5] S. T. Bramwell and M. J. P. Gingras, Science **294**, 1495 (2001).
[6] J. S. Gardner, B. D. Gaulin, A. J. Berlinsky, P. Waldron, S. R. Dunsiger, N. P. Raju, and J. E. Greedan, Phys. Rev. B **64**, 224416 (2001).
[7] J. S. Helton *et al.*, Phys. Rev. Lett. **98**, 107204 (2007).
[8] N. Hanasaki, K. Watanabe, T. Ohtsuka, I. Kezsmarki, S. Iguchi, S. Miyasaka, and Y. Tokura, Phys. Rev. Lett. **99**, 086401 (2007).
[9] I. Kezsmarki, N. Hanasaki, K. Watanabe, S. Iguchi, Y. Taguchi, S. Miyasaka, and Y. Tokura, Phys. Rev. B **73**, 125122 (2006).
[10] Y. Taguchi, Y. Oohara, H. Yoshizawa, N. Nagaosa, and Y. Tokura, Science **291**, 2573 (2001).
[11] N. Hanasaki, K. Sano, Y. Onose, T. Ohtsuka, S. Iguchi, I. Kézsmárki, S. Miyasaka, S. Onoda, N. Nagaosa, and Y. Tokura, Phys. Rev. Lett. **100**, 106601 (2008).
[12] I. Mirebeau, A. Apetrei, J. Rodríguez-Carvajal, P. Bonville, A. Forget, D. Colson, V. Glazkov, J. P. Sanchez, O. Isnard, and E. Suard, Phys. Rev. Lett. **94**, 246402 (2005).
[13] P. Dalmas de Réotier, A. Yaouanc, L. Keller, A. Cervellino, B. Roessli, C. Baines, A. Forget, C. Vaju, P. C. M. Gubbens, A. Amato, and P. J. C. King, Phys. Rev. Lett. **96**, 127202 (2006).
[14] F. Bert, P. Mendels, A. Olariu, N. Blanchard, G. Collin, A. Amato, C. Baines, and A. D. Hillier, Phys. Rev. Lett. **97**, 117203 (2006).
[15] B. D. Gaulin, J. N. Reimers, T. E. Mason, J. E. Greedan, and Z. Tun, Phys. Rev. Lett. **69**, 3244 (1992).
[16] A. Apetrei, I. Mirebeau, I. Goncharenko, D. Andreica, and P. Bonville, Phys. Rev. Lett. **97**, 206401 (2006).
[17] S. R. Dunsiger *et al.*, Phys. Rev. B **54**, 9019 (1996).
[18] M. J. P. Gingras, B. C. den Hertog, M. Faucher, J. S. Gardner, S. R. Dunsiger, L. J. Chang, B. D. Gaulin, N. P. Raju, and J. E. Greedan, Phys. Rev. B **62**, 6496 (2000).
[19] I. Mirebeau, P. Bonville, and M. Hennion, Phys. Rev. B **76**, 184436 (2007).
[20] Y. Chapuis, A. Yaouanc, P. D. Reotier, S. Pouget, P. Fouquet, A. Cervellino, and A. Forget, J. Phys.: Condens. Matter **19**, 446206 (2007).
[21] J. van Duijn, K. H. Kim, N. Hur, D. Adroja, M. A. Adams, Q. Z. Huang, M. Jaime, S.-W. Cheong, C. Broholm, and T. G. Perring, Phys. Rev. Lett. **94**, 177201 (2005).
[22] C. H. Booth, J. S. Gardner, G. H. Kwei, R. H. Heffner, F. Bridges, and M. A. Subramanian, Phys. Rev. B **62**, R755 (2000).
[23] A. Keren and J. S. Gardner, Phys. Rev. Lett. **87**, 177201 (2001).